HHS Public Access

Author manuscript

Circ Res. Author manuscript; available in PMC 2022 September 17.

Published in final edited form as:

Circ Res. 2021 September 17; 129(7): 702–716. doi:10.1161/CIRCRESAHA.120.318271.

Dach1 Extends Artery Networks and Protects Against Cardiac Injury

Brian Raftrey[1], **Ian Williams**[1], **Pamela E. Rios Coronado**[1], **Xiaochen Fan**[1], **Andrew H. Chang**[1,4], **Mingming Zhao**[2,6], **Robert Roth**[1], **Emily Trimm**[1], **Raquel Racelis**[1], **Gaetano D'Amato**[1], **Ragini Phansalkar**[1,3], **Alana Nguyen**[5], **Timothy Chai**[5], **Karen M. Gonzalez**[1,5], **Yue Zhang**[1], **Lay Teng Ang**[5], **Kyle Loh**[4,5], **Daniel Bernstein**[2,6], **Kristy Red-Horse**[1,5,6]

[1]Biology, Stanford University, Stanford, CA, 94305;

[2]Division of Pediatric Cardiology, Department of Pediatrics, Stanford University School of Medicine, Stanford, CA, 94305;

[3]Genetics, Stanford University School of Medicine, Stanford, CA, 94305;

[4]Developmental Biology, Stanford University School of Medicine, Stanford, CA, 94305;

[5]Institute for Stem Cell Biology and Regenerative Medicine, Stanford University School of Medicine, Stanford, CA 94305, USA,

[6]Stanford Cardiovascular Institute, Stanford University School of Medicine, Stanford, CA 94305, USA.

Abstract

Rationale: Coronary artery disease (CAD) is the leading cause of death worldwide, but there are currently no methods to stimulate artery growth or regeneration in diseased hearts. Studying how arteries are built during development could illuminate strategies for re-building these vessels during ischemic heart disease. We previously found that *Dach1* deletion in mouse embryos resulted in small coronary arteries. However, it was not known whether *Dach1* gain-of-function would be sufficient to increase arterial vessels and whether this could benefit injury responses.

Address correspondence to: Kristy Red-Horse, 318 Campus Drive, Room E380, Stanford, CA 94305, USA, kredhors@stanford.edu.

AUTHOR CONTRIBUTIONS

B.R., I.W., D.B., and K.R conceptualized the study and wrote the manuscript. B.R., I.W., P.R., X.F., E.T., and H.Y.Z. performed experiments and computational analysis. B.R., M.Z., and R.R. performed cardiac injury studies. A.N., T.C., L.T.A., and K.L. assisted with experiments. A.C. designed the *Dach1*^{OE} mouse. R.P., G.D., and K.G. assisted with the FACS procedure. K.R., D.B., and K.L. provided recourses.

DISCLOSURES

None

SUPPLEMENTAL MATERIALS

Expanded Materials & Methods

Online Figures I–V

Online Tables I–II

References 26–32

Objective: We investigated how *Dach1* overexpression in endothelial cells affected transcription and artery differentiation, and how it influenced recovery from myocardial infarction (MI).

Methods and Results: *Dach1* was genetically overexpressed in coronary endothelial cells (ECs) in either developing or adult hearts using *ApjCreER.* This increased the length and number of arterial end branches expanded arteries during development, in both the heart and retina, by inducing capillary ECs to differentiate and contribute to growing arteries. Single-cell RNA sequencing (scRNAseq) of ECs undergoing *Dach1*-induced arterial specification indicated that it potentiated normal artery differentiation, rather than functioning as a master regulator of artery cell fate. ScRNAseq also showed that normal arterial differentiation is accompanied by repression of lipid metabolism genes, which were also repressed by Dach1. In adults, *Dach1* overexpression did not cause a statistically significant change artery structure prior to injury, but increased the number of perfused arteries in the injury zone post-MI.

Conclusions: Our data demonstrate that increasing *Dach1* is a novel method for driving artery specification and extending arterial branches, which could be explored as a means of mitigating the effects of CAD.

Graphical Abstract

Stimulating coronary artery growth can prevent, or aid in recovery after myocardial infarction. However, the pathways which regulate artery cell specification from their capillary precursors are not fully known. Here, we show that overexpression the nuclear transcriptional regulator, Dach1, can induce artery endothelial cell specification during embryonic and postnatal development. Not only do these findings describe a previously unrecognized specification pathway, but they also relate a new genetic strategy that increases coronary artery abundance far beyond what has been reported in a developmental setting. In addition, we found through single cell RNA sequencing that Dach1 mediated specification was accompanied by downregulation of lipid transport, which has not been liked to artery specification previously. Given that artery growth can affect the response to myocardial infarction, we tested the effect of Dach1 overexpression on a coronary artery ligation ischemia model in mice. This revealed that Dach1 overexpressors had greater survival and heart function after ligation. Further studying how the transcriptional and cellular changes induced by Dach1 contribute to protection from myocardial infarction could improve our ability to treat coronary artery disease in humans.

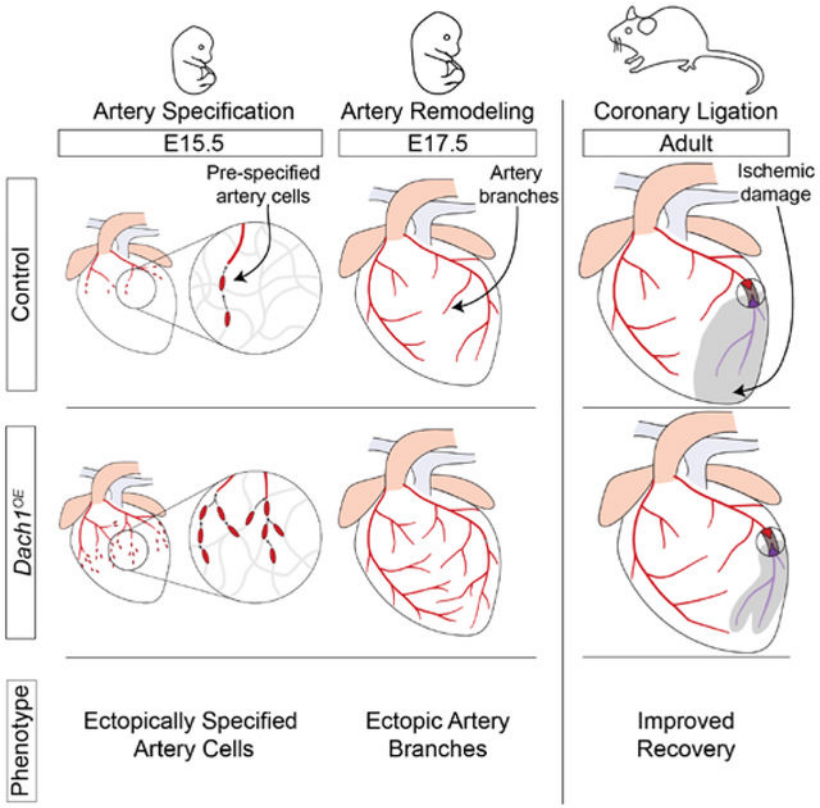

Subject Terms:

Angiogenesis; Coronary Circulation; Developmental Biology; Genetically Altered and Transgenic Models; Vascular Biology

INTRODUCTION

Heart disease is the leading cause of death and is triggered by atherosclerotic coronary artery disease (CAD)[1]. Although lifesaving interventions exist, there are significant limitations, highlighting the need for novel treatments[2]. Given that heart disease is caused by dysfunctional arteries, a promising strategy would be to regenerate diseased coronary arteries.

Coronary vessels are composed of three vessel subtypes—arterial, venous, and capillary, the latter of which is most numerous and where tissue oxygen exchange occurs. Research has identified pro-angiogenic proteins, such as vascular endothelial growth factor (VEGF), that stimulate capillary growth[3]. However, clinical trials applying these factors to treat ischemic heart disease have largely failed[4]. Some suggest that a beneficial treatment would need to grow arterial vessels in addition to capillary microvasculature[5,6]. However, the factors that stimulate the growth of functioning arterial vessels in an established adult vascular bed, such as the heart, are not completely understood[7].

We previously demonstrated a requirement for the transcription factor *Dach1* during coronary artery development. *Dach1* deletion reduced coronary artery diameter by 33%[8]. Mechanistically, Dach1 was important for artery development because it potentiated blood flow-guided EC migration into growing arteries through upregulating *Cxcl12* expression.

While *Dach1* deletion stunted coronary artery growth by impairing EC migration, it was unclear whether *Dach1* had additional roles. Coronary artery development starts with immature capillary plexus formation in heart muscle[9]. Then, individual ECs within this plexus differentiate into arterial ECs[10]. These “pre-artery cells” are initially intermixed throughout the plexus, but after arterial specification, migrate together to form large arteries. Whether *Dach1* is also involved in these other arteriogenic processes is unknown.

Using gain-of-function experiments, we found that, in addition to its effect on migration, Dach1 also increased artery EC fate specification, in both the developing heart and retina. *Dach1* overexpression in plexus and capillary ECs potentiated pre-artery specification and lengthened artery branches. scRNAseq showed that *Dach1* did not widely induce the expression of known artery cell fate determinants, but rather enhanced arterialization in EC subpopulations that are normally receptive to arterial specification. Finally, overexpression in adult hearts improved survival and cardiac function following MI. Our results indicate that upregulation of *Dach1* could be a target for therapeutically regenerating arterial blood vessels.

METHODS

Data Availability.

All scRNA seq data including raw reads and Seurat processed data are publicly available at GEO (GSE179857).

Details of the experimental methods are available in the Data Supplement.

Please see the Major Resources Table in the Supplemental Materials.

For the majority of experiments, female $Dach1^{OE}/Dach1^{OE}$ mice were crossed to *ApjCreER* males to generate $Cre{-};Dach1^{OE}/+$ or $Cre{+};Dach1^{OE}/+$ animals used as either controls or Dach1 overexpressors respectively, upon administration of Tamoxifen. Tissue collection, fixation, immunostaining, and imaging were performed on embryonic hearts[10], postnatal hearts[11], retinas[8], and adult hearts[12] as previously described.

To prepare samples for single cell RNA seq, embryonic hearts were enzymatically digested, and the single cell suspension was FACS sorted to remove red blood cells and enrich for endothelial cells. Single cell sequencing was done using the 10X single cell V3 platform and analysis was performed using Cell Ranger, R, and Seurat[13].

Coronary artery ligation experiments were done by opening the chest cavity and placing a 7–0 silk suture around the left anterior descending artery (LAD), with occlusion verified by blanching of the underlying myocardium. Transthoracic echocardiograms were then used

to assess cardiac function. Following fixation, ligated hearts were embedded in paraffin, sectioned, and stained with Masson's Trichrome.

RESULTS

Dach1 overexpression increases artery specification and branching in the heart.

Since *Dach1* deletion impairs artery development[8], we hypothesized that increasing it would promote artery growth. Thus, we generated a transgenic mouse that would inducibly overexpress *Dach1*. A transgene containing the *CAG* promoter upstream of a *Flox-Stop-Flox-Dach1-IRES-EGFP* sequence was inserted into the *ROSA26* locus (Fig. 1A). We next crossed these with *ApjCreER*, which is expressed in ECs of the developing coronary capillary plexus and veins but not in differentiated arterial ECs[14]. Cre induction with Tamoxifen resulted in excision of the transcriptional stop sequence and permanent co-expression of *Dach1* and EGFP in plexus ECs. We observed high levels of Cre-dependent recombination and *Dach1* expression inferred from EGFP expression (Fig. 1B) and anti-Dach1 immunofluorescence (Fig. 1C). Tamoxifen was given to experimental (*ApjCreER;Dach1^{OE}*) and control (Cre-negative *Dach1^{OE}*) mice, but we verified that neither transgene affected coronary development in the absence of Tamoxifen (data not shown). This tool was then used to explore the effects of *Dach1* overexpression on artery formation.

We induced *Dach1^{OE}* at embryonic day (e) 13.5, when arterial EC differentiation normally begins, and harvested embryos at e15.5 (Fig. 1D). At this time, single, pre-artery ECs that have differentiated within the immature capillary plexus have begun to coalesce into coronary arteries that can be morphologically distinguished[10]. The effect of *Dach1^{OE}* was assessed by immunostaining for ECs (VE-cadherin) and the arterial EC marker Connexin 40 (CX40). CX40-positive artery ECs in control hearts were in larger diameter arterial vessels and the capillary plexus as cells that have been specified as arterial but have not yet assembled into the artery, i.e. pre-artery cells (Fig. 1E, upper panels). In *Dach1^{OE}* mutants, we observed an increase in the number of capillary plexus ECs expressing CX40 (Fig. 1E, lower panels). Quantifying the area of each heart covered by CX40 positive ECs revealed a 71% increase in *Dach1^{OE}* hearts (Fig. 1F). These results indicate that *Dach1* overexpression stimulates pre-artery specification in ECs within the capillary plexus. We did not find statistically significant differences in proximal coronary artery diameters (Fig. 1G), heart sizes (Fig. 1H), and the number of ECs within the myocardium (Fig. 1I). We concluded that *Dach1* overexpression increased the abundance of arterialized ECs without grossly affecting cardiac development.

We next analyzed artery morphology 4 days post-induction at e17.5 when arteries are more mature (Fig. 2A). Immunostaining for CX40 revealed that distal branches were more numerous, while diameters of proximal branches were not different (Fig. 2B). Additional branches expressed other artery markers (*Jag1*, CX37) (Online Fig. IA–C) and received blood flow as assessed by fluorescent lectin perfusions (Online Fig. ID, E). EC coverage was not grossly affected as assessed by VE-cadherin staining (Fig. 2B). Summing the lengths of all CX40+ vessels revealed a 79% increase in artery lengths (Fig. 2C) and counting junctions showed a 334% increase in branching (Fig. 2D). No statistically significant difference in primary artery diameters was found between groups (Fig. 2E). This suggests that the

increased pre-artery specification observed at e15.5 precedes the development of excessive distal artery branches at e17.5.

To extend our analysis beyond embryonic development, we induced *Dach1* at postnatal day (P) 0 and analyzed arteries at P6 (Fig. 2F). Similar to embryonic hearts, distal artery branches were more numerous (Fig. 2G, H) with increased branching (Fig. 2I) in the watershed area between the right and left coronary arteries. Diameters of proximal coronary branches were not significantly different (Fig. 2J).

We next determined whether the increase in artery branches resulted from Dach1 activity in capillary plexus or arterial ECs. Above, *ApjCreER* will only induce $Dach1^{OE}$ in the capillary plexus, but overexpression will be maintained in the arteries that differentiate from these cells. To test whether *Dach1* has the same effects when expressed exclusively in artery ECs, we analyzed *CX40CreER;*$Dach1^{OE}$ e15.5 embryos dosed with Tamoxifen at e13.5 (Fig. 2K). In contrast to *ApjCreER* induction, there was no statistically significant difference in artery abundance or width in *CX40CreER;*$Dach1^{OE}$ animals (Fig. 2L–N). We conclude that *Dach1* increases arterial branching through its activity in capillary plexus ECs.

Dach1 overexpression increases retinal arteries cell autonomously,

We next used the retina to investigate whether *Dach1*-induced artery specification occurs in other vascular beds. *Dach1* was overexpressed in all ECs using *Cdh5CreER* and a high dose of Tamoxifen at P0. VE-cadherin and CX40 expression revealed arterial morphology at P7 (Fig. 3A, and Online Fig. IH). There was a 2.5 fold increase in the combined length of all CX40-labeled arteries in $Dach1^{OE}$ retinas (Fig. 3B, C). Interestingly, arterial branches often crossed paths with veins, suggesting a breakdown of arterial-venous repulsion (Fig. 3D, E). These data show that *Dach1* is capable of extending arterial networks in a vascular bed other than the heart.

There were differences between the heart and retinal vascular beds. First, despite previous reports[15], we did not observe any CX40-positive cells outside arteries within the capillary plexus in either control or $Dach1^{OE}$ retinas, which is a hallmark of pre-artery cells in the heart. Artery pre-specification occurs in the retina, but at the tip cell location, i.e. the migrating front of the growing vasculature[16,17]. Our data indicated that CX40 does not label pre-specified arterial ECs in the retina. Second, $Dach1^{OE}$ stunted angiogenesis in retinas as demonstrated by decreased outward expansion (Fig. 3B). This discordance in phenotypes likely results from the timing of $Dach1^{OE}$ induction in the two models. In the retina, *Dach1* was overexpressed prior to the initiation of retinal angiogenesis while, in the heart, expression was induced after the coronary plexus was established. The retinal experiments also used a more widespread Cre line (*Cdh5CreER*) with a longer time after Tamoxifen induced recombination. Both of these factors likely contribute to a more severe angiogenic phenotype in the retina. However, the shared phenotype is increased artery branching.

We next investigated whether *Dach1*-induced arterialization was cell autonomous. Low dose Tamoxifen at P0 induced mosaic $Dach1^{OE}$ recombination in 2.3 ± 2.0% of retinal ECs (Fig. 3F) where $Dach1^{OE}$ was tracked by EGFP expression (Fig. 1A). *ROSA26;tdTomato* Cre reporter mice were used as a control. The localization of ECs to arteries, capillaries, or

veins was determined at P6 and P9. Vessel subtypes were distinguished morphologically using VE-cadherin staining. At P6, the majority of tdTomato^{+} control cells were within capillary vessels while the remaining were distributed among arteries, veins, and tip cells, the latter of which are at the migrating front of the developing vasculature (Fig. 3G). When compared to controls, the number of *Dach1^{OE}* cells in arteries and at the tip position more than doubled while those in veins decreased (Fig. 3H, I). As pre-specified arterial ECs localize to tips in the retina[16,17], the accumulation of *Dach1^{OE}* ECs here is evidence that it contributes to arterial pre-specification in the retina. Analyzing cellular distributions at P9 showed that *Dach1^{OE}* cells no longer accumulated at tips, but became even more enriched in arteries (Fig. 3J–L). These data demonstrate that *Dach1* overexpression directly causes ECs to follow a path towards arterialization in a cell autonomous fashion.

Dach1 shifts the endothelial specification trajectory towards arterialization.

The above data and that in Chang et al. contain multiple loss- and gain-of-function scenarios demonstrating that Dach1 is critical for proper coronary artery differentiation. However, its expression pattern does not suggest a simple explanation as to how. Specifically, Dach1 is expressed in most coronary ECs arising from the sinus venosus as soon as they appear on the heart[148]. However, only a subpopulation of Dach1+ cells yields arteries. One potential explanation is our observation that protein levels (and possibly transcript levels) are heterogeneous among expressing cells, both in vivo and in vitro, and they are dramatically decreased in large arteries due to high laminar shear stress[8].

How does a transcription factor expressed in most coronary ECs drive differentiation of a small subpopulation into arteries? To address this question, we performed single cell transcriptomics on *Dach1^{OE}* cardiac ECs. Either *tdTomato* (control) or *Dach1^{OE}* was induced in plexus ECs at e13.5, and cells were isolated at e15.5 by FACS followed by scRNAseq using the 10X Genomics platform (Fig. 4A). Sequencing and alignment parameters served as quality controls (Online Fig. IIA). Low-quality cells were excluded based on total number of reads, number of genes per cell, and percentage of reads aligned to mitochondrial genes (Online Fig. IIB, C). To focus our analysis of coronary ECs, we also removed the endocardial cell population that lines the heart lumen (Online Fig. IID).

Datasets were integrated[13] and projected into 2-dimensional space using the uniform manifold approximation and projection (UMAP) algorithm. Unsupervised graph-based clustering partitioned ECs into 2 artery (Art1 and Art2), 1 vein, and 5 capillary clusters (Fig. 4B), which were annotated based on known markers (Fig. 4C). Gene expression suggested that Art1 was comprised of less mature arterial ECs whereas Art2 were more mature. Specifically, Art2 largely contained increased expression of Art1 markers with the addition of a few mature arterial EC markers such as *Jag1* and *Cxcl12* (Fig. 4C [box], and Online Fig. IIIA). All Art1 ECs expressed *Cxcr4* but showed heterogeneous expression of *Cx37* and were negative for *Jag1,* suggesting this cluster is a mix of arterially-skewed capillary ECs and pre-artery ECs (Online Fig. IIIA).

Although distinct clusters, the UMAP topography and gene expression patterns indicated that EC subtypes exist along a continuum, rather than as completely distinct states (Online Fig. IIIB). This was particularly evident when projecting cells on an axis of arterial-venous

identity (Online Fig. IIIC), and was consistent with previous analyses showing that brain and heart capillary ECs exist along a continuum, even in adults[10,18]. Nonetheless, cells from all clusters were in both genotypes (Fig. 4B, D), suggesting that *Dach1*^{OE} does not create a new cell identity or transcriptional state not normally present.

We also observed that cell cycle phase, inferred from the enrichment of phase-specific genes, was a major source of variability. Most capillary ECs (clusters Cap1-4) were either in S or G2/M phase (i.e., cycling) while one capillary cluster (Cap5) and the artery and vein clusters were in G0/G1 (i.e. non-cycling; Fig. 4E). In summary, scRNAseq allowed us to isolate artery, vein, and capillary (cycling and non-cycling) ECs from control and *Dach1*^{OE} hearts for subsequent transcriptomic analysis.

Although all EC subtypes were in both genotypes, *Dach1*^{OE} altered the relative number of ECs within specific clusters. *Dach1*^{OE} induced a 48% increase in arterial ECs while decreasing cycling capillary ECs by 21% (Fig. 4F). This corroborated our observation of increased CX40^{+} arterial ECs in developing hearts. Importantly, it further demonstrated that ECs are not only CX40^{+}, but also express a full arterial transcriptomic program.

We next investigated how *Dach1*^{OE} increased arterial specification of capillary ECs. One hypothesis is that Dach1 induces expression of arterial fate determinants in all capillary ECs. Notch transcription factors are the most well recognized artery cell fate determinants described to date[19]. Examining differentially expressed genes (DEGs; LogFC > 0.25) between *Dach1*^{OE} and control in each cluster, we found that Dach1 overexpression did not result in statistically significant changes in Notch pathway genes, or any other validated artery marker, in capillary subpopulations even though it was overexpressed in virtually all ECs (Fig. 4G, and Online Fig. IIIB). Instead, Dach1 increased arterial genes in select clusters, including arterial ECs (Fig. 4G, and Online Fig. IIIB). This observation suggests that Dach1's arterializing capability is restricted to certain EC subtypes and/or involves upregulating previously uncharacterized arterial fate determinants.

To determine which EC subtypes are sensitive to arterialization, we calculated artery scores, which were determined by measuring each cell's enrichment of the genes that defined Art2 in controls (Online Table I, II). Consistent with ECs existing along a continuum, control cells were distributed along the entire artery score spectrum while *Dach1*^{OE} ECs were shifted towards higher artery scores (Fig. 5A). This is likely attributable to elevated artery scores in artery clusters, as artery scores were not statistically significantly different in other clusters after adjusting for Sidak's multiple comparison test (Fig. 5B, and Online Fig. IVA). This is consistent with the specific expansion of *Cx40* in Art1 as shown in Fig. 4G. These data indicate that Dach1 upregulates arterial genes specifically in arterial skewed capillary, pre-artery, and arterial ECs.

To determine the effects of *Dach1*^{OE} on the arterial specification trajectory, we first needed to delineate this trajectory in control ECs. Trajectory analysis using monocle 3[20] showed that Cycling cap, Cap5^{G1}, Art1, and Art2 clusters were transcriptomically connected in series while veins branched off of Cap5^{G1} (Fig. 5C top panel). We then ordered this lineage connection by developmental stage using CytoTRACE (Cellular Trajectory Reconstruction

Analysis using gene Counts and Expression)[21]. This method predicts cellular differentiation potential by calculating the expression of genes that correlate with the number of genes expressed per cell[21]. CytoTRACE scored the Cycling cap cluster as the least differentiated followed by Vein, Cap5^{G1}, Art1, and then finally Art2 as most differentiated (Fig. 5D top panel, and E).

Because the above data were collected from a single time point, we sought additional evidence for this developmental trajectory. First, we determined the pattern of lineage tracing labels among different EC subtypes. These data showed that *Apj*, the promoter that drives Cre-mediated *tdTomato* (control) and *EGFP* (*Dach1*^{OE}) expression, is only expressed in Cycling cap, Cap5^{G1}, and Vein ECs (Fig. 5G). This was supported by capillary-specific Cre recombination in *ApjCreER* hearts 9 hours after a Tamoxifen dose (Online Fig. IVB, C). Thus, the non-artery EC subtypes initially expressed *tdTomato* or *EGFP* following Cre induction at e13.5. However, after two days, *tdTomato* (control) and *EGFP* (*Dach1*^{OE}) lineage expression was seen in arterial ECs, indicating that the artery clusters arise from *Apj*-positive capillary and/or vein ECs (Fig. 5H). We also integrated this dataset with previously generated e12.5 and e14.5 datasets[10]. Quantifying the ratio of cells at each time point showed that higher proportions of Art1 (less mature) precede higher Art2 (more mature) proportions (Fig. 5I). Considering all of these findings, we propose that the artery trajectory includes the following steps: 1) exit of proliferating capillary ECs from the cell cycle and differentiation to a non-cycling capillary subtype (Cap5^{G1}), 2) initial pre-artery/artery specification (Art1), and 3) full differentiation into mature arterial ECs (Art2) (Fig. 5J).

We next determined how *Dach1*^{OE} influences this developmental progression. Trajectory analyses revealed that Cap5^{G1} ECs in *Dach1*^{OE} are more linearly connected with arterial ECs (Fig. 5C lower panel). *Dach1*^{OE} Cap5^{G1} and Art1 cells were significantly more differentiated as scored by CytoTRACE (Fig. 5D lower panel, and F), while the differentiation state of Cycling cap, Vein, and Art2 ECs were not significantly different after adjusting for Bonferroni's multiple comparison test (Fig. 5D, F). These data suggest Dach1 is not an arterial cell fate determinant per se, but potentiates arterialization in receptive cells such as Cap5^{G1} and pre-artery cells in Art1 (Fig. 5J).

Gene expression changes in Dach1^{OE}

To investigate which genes *Dach1*^{OE} might regulate to influence arterialization, we first compared DEGs between *Dach1*^{OE} and controls with genes that were positively or negatively enriched in control artery ECs. Each cluster had between 50–160 DEGs above a .25 log fold change (Fig. 6A). 38% of the Vein and 34% of the Cycling cap DEGs that were upregulated in *Dach1*^{OE} were on the list of 498 genes whose increase defined the Artery 2 cluster in control hearts, i.e. "arterial EC genes" (Fig. 6B, and Online Table I). More than 50% of the upregulated DEGs in *Dach1*^{OE} Cap5^{G1}, Art 1, and Art 2 were also arterial EC genes (Fig. 6B). In contrast, a much smaller percentage of the DEGs upregulated in *Dach1*^{OE} were on the list of 436 that were downregulated in control arterial ECs, i.e. "non-arterial EC genes" (Fig. 6B, and Online Table II). When considering genes downregulated by *Dach1*^{OE}, there were much lower percentages of overlap with arterial EC

genes and non-arterial EC genes, and there was no differential pattern between the two types (Fig. 6C). This suggests that all *Dach1*^{OE} ECs may contain some level of arterial priming towards through the induction of genes not previously correlated with artery fate, and that there is a greater induction of artery genes rather than repression of non-artery genes.

Since lineage data suggested Cap5 cells were the direct artery progenitors (Fig. 5C–H) and differentiation state of this cluster was affected by *Dach1*^{OE} (Fig. 5F), the genes changed in this subpopulation could influence differentiation. Upregulated DEGs included genes that stimulate artery differentiation such as *Gja4* (*CX37*)[22] and *Sox7*[23], or artery remodeling such as *Cxcl12*[8] (Fig. 6D). Unexpectedly, downregulated DEGs included several lipid transport and metabolism genes (Fig. 6E). Thus, we investigated additional lipid metabolism and signaling pathways and found that genes associated with lipid transport, lipid oxidation and eicosanoid metabolism were significantly downregulated by *Dach1*^{OE} (Fig. 6F, and Online Fig. IVD–G). The change in one of these, *Fabp4*, was validated at the protein level in both embryonic and adult hearts (Fig. 6G–J). Although not typically linked to artery development, these data suggest suppression of lipid metabolism might be involved.

Since arterial specification is linked to cell cycle exit[10,22], we noted that *Cdkn1c* expression, a cell cycle inhibitor, was upregulated by *Dach1*^{OE} (Fig. 6D). EdU incorporation experiments marked the number of cells entering S-phase to assess whether Dach1 decreased cell cycling. Analyses focused on non-arterial regions to avoid confounding results due to cell cycle exit being linked to arterial differentiation. There was no statistically significantly difference in EdU incorporation in *Dach1*^{OE} vessels where arterial differentiation does not occur (Online Fig. IVH). It was decreased within intramyocardial regions, but this could be due to the increased arterial differentiation at that location (Online Fig. IVI). EdU incorporation was not significantly different in the retina (Online Fig. IVJ). Thus, although not affecting S-phase entry in all cells, upregulation of *Cdkn1c*, could potentiate cell cycle arrest in the presence of other artery differentiation signals.

Dach1^{OE} scRNAseq DEG lists were cross-referenced with a previously generated bulk RNAseq dataset from cultured human coronary artery endothelial cells overexpressing *Dach1* (*Dach1*-HCAECs)[8]. 26.4% of the genes upregulated in *Dach1*^{OE} mouse coronary ECs were also upregulated in *Dach1*-HCAECs, and 30.7% of downregulated genes overlapped with those downregulated in cultured cells (Fig. 6K). Notable genes regulated in both systems were *Cxcl12, Aqp1, Cdkn1c,* and lipid transport genes (Fig. 6K). This analysis identified genes regulated by *Dach1*^{OE} in both mouse ECs in vivo and cultured human ECs.

As mentioned above, although Dach1 is expressed in most coronary ECs, protein levels vary from cell-to-cell[8], which in scRNAseq data results in different levels of mRNA and includes cells with none detected at all (Fig. 4G). Given the protein expression patterns and detection limits of scRNAseq, the lack of transcripts likely reflects low expression instead of absence. This allowed us to investigate whether the genes induced by *Dach1*^{OE} reflect the genes that are endogenously regulated by higher levels of Dach1. Cells from control hearts only were used to correlate presence of *Dach1* mRNA in scRNAseq data to the expression of all other genes. Identifying the top 500 genes positively and negatively correlated with endogenous *Dach1* and comparing those to *Dach1*^{OE} DEGs revealed strong overlaps (Fig.

6L). Prominent on these lists were arterial EC and non-arterial EC genes, such as *Aqp1* and lipid transporters, respectively. This supports the idea that overexpressing *Dach1* affects similar transcriptional programs as endogenous *Dach1*, and that this transcription factor regulates artery and lipid transport genes in multiple settings.

Dach1 overexpression supports recovery post-MI.

We next investigated whether *Dach1* overexpression improved outcomes following myocardial infarction (MI). Left anterior descending coronary arteries were permanently ligated in 12-week-old adult mice with *ApjCreER*-induced *Dach1* overexpression in capillary and venous ECs for 6 weeks prior to injury (Online Fig. VA). Quantification showed *Dach1* overexpression in 64.5±14% of coronary ECs (Online Fig. VB).

MI resulted in 43.3% survival for control animals (Fig. 7A). Most fatalities occurred within 10 days post-MI while $Dach1^{OE}$ mice exhibited a 90.6% survival rate (Fig. 7A). Echocardiography revealed that $Dach1^{OE}$ mice had higher ejection fractions than controls over the course of the study (Fig. 7B). A control experiment using the same genotypes without Tamoxifen showed that this rescue effect was not due to the *ApjCreER* transgene (data not shown).

Histology at 4 weeks revealed reduced fibrosis in $Dach1^{OE}$ (Fig. 7C, D). In 92% of WT mice, fibrotic scars extended the full thickness of the myocardium, whereas this pattern was seen in only 59% of $Dach1^{OE}$ hearts (Fig. 7E). In hearts without full thickness scars, fibrosis was limited to mid-myocardial regions (Fig. 7C, E). Mice with no scar were excluded from analysis due to technical failure. Measuring myocardial thickness at sequential points around the entire heart revealed an increased thickness in $Dach1^{OE}$ left ventricles (Fig. 7F).

We investigated whether improvements were due to arterial changes. Measuring the percent area stained by the artery marker smooth muscle actin (SMA) 6 weeks after Tamoxifen but prior to injury did not reveal a statistically significant difference between control and $Dach1^{OE}$ (Fig. 7G), which was consistent with qualitative analyses of whole mount images (Online Fig. VC). 4-weeks after injury, $Dach1^{OE}$ hearts with mid-myocardial scars, had a higher SMA+ areas, indicating increased arterialization in hearts with the best recovery (Fig. 7H). This effect did not appear to be driven by the hearts with mid-myocardial scars merely having more intact myocardium since, unexpectedly, scarred regions still contained many arteries (Fig. 7H). To compare infarct sizes, fluorescent lectin was injected into ventricles post-mortem to perfuse the coronary system either at 2 hours or 5 days after coronary ligation. At 2 hours, infarct sizes were not significantly different (Fig. 7I). 5 days post-MI, $Dach1^{OE}$ hearts contained isolated perfused vessels running from the border zone into infarcted tissue in 60% of the samples (Fig. 7J). Whether these partially perfused regions would increase with longer perfusion techniques or whether they would be enough to explain the observed myocardial protection will be the subject of future studies. Together, these patterns indicate that adult overexpression of *Dach1* does not change pre-existing artery structure, but increases arteries and affects perfusion to the infarcted area in the days following injury.

To observe whether more dramatic effects on artery structure could be obtained by over expressing *Dach1* from earlier stages, *ApjCreER;Dach1*^{OE} mice were dosed with Tamoxifen at e13.5 and kept until adulthood. All treated mice survived, but with enlarged hearts (Online Fig. IF). Visualization of adult artery trees indicated that the extra artery branching phenotype was either lost or less extensive in adults (Online Fig. IG).

In addition to arterial expansion after injury, unrelated gene expression changes could also underly the protective injury response. *Dach1* suppressed lipid transport genes, and recent studies showed that decreasing the heart's utilization of fatty acids promotes adult cardiomyocyte proliferation and heart regeneration[24]. It is possible that changes in endothelial lipid transport to cardiomyocytes could similarly contribute to improved outcomes after MI. Blood profiles of uninjured mice revealed baseline decreases in total cholesterol and HDL cholesterol in the blood of *Dach1*^{OE} mice, suggesting misregulation of systemic lipid pathways (Online Fig. V D, E). It will be interesting to ascertain any functional consequences in future studies.

DISCUSSION

Coronary artery ECs differentiate from capillaries; however, transcriptional regulators of this transition remain incompletely understood. We found that overexpression of *Dach1* drove ectopic arterial EC specification in coronary capillaries. Extra arterial ECs contributed to artery remodeling to create longer, more branched arterial networks, which was also detected in the retina. ScRNAseq revealed that *Dach1*^{OE} suppressed lipid transport genes in all ECs, but upregulated arterial genes specifically in capillaries on the arterial side of the artery-vein vein continuum and in pre-artery and arterial populations. Finally, *Dach1* overexpression in adults improved survival and heart function following MI, which was accompanied by an increase in arteries and perfusion that occurred only in the days following injury.

Mosaically expressing *Dach1*^{OE} in retinal ECs resulted their localization first to the tip cell location and then to arteries, supporting previous data proposing that Dach1 supports artery development by potentiating EC migration against the direction of blood flow into growing arteries[8]. In the retina, cells at the tips of the growing angiogenic front are selected as pre-artery cells and eventually change direction to migrate into developing arteries[16,17,25]. These data align Dach1 overexpression with this process, and demonstrate the it potentiates arterialization in a cell autonomous manner.

Endogenously, *Dach1* is widely expressed in coronary ECs in both embryos and adults, although levels are downregulated in the mature artery[8]. This widespread, high expression of *Dach1* in capillaries and veins, suggests that: 1) Its ability to induce arterialization is dependent on the context of the particular EC and 2) Dach1 may have functions independent of inducing artery genes. During arterialization, we propose that Dach1 either collaborates with a co-factor with a more restricted expression pattern or functions to lower the threshold for arterialization signals present at specific locations in the tissue.

Given the developmental effect of *Dach1* overexpression, we hypothesized that it could enhance recovery from ischemic injury. Animals with *Dach1* overexpression in coronary capillary and vein ECs experienced increased ejection fraction and survival. Notable was the pattern of myocardial fibrosis in $Dach1^{OE}$—damaged myocardium was restricted to an intramyocardial region and covered by surviving myocardium on both the epicardial and endocardial faces. While overexpression did not result in statistically significant changes in arterial structure before injury, we found evidence for increased artery growth after infarction that benefited re-perfusion. Thus, injury may reactivate pathways not present in healthy tissue that allow Dach1 to induce artery differentiation. This work supports further investigation of Dach1 as a potential therapeutic target aimed at enhancing revascularization of ischemic hearts.

Supplementary Material

Refer to Web version on PubMed Central for supplementary material.

SOURCES OF FUNDING

K.R. is a New York Stem Cell Foundation – Robertson Investigator. K.R. is also supported by the NIH (R01-HL128503). B.R. is supported by NIH (5 F31 HL147410-02), NSF GRFP. I.W. is supported by T32HL098049. P.R. is supported by NIH (T32GM007276), NSF GRFP. R.P. is supported by an AHA graduate fellowship. A Stanford CVI seed grant funded MI experiments. D.B is supported by the Department of Defense CMDRP in Congenital Heart Disease W81XWH-16-1-0727. We thank all members of the Red-Horse lab for technical and intellectual support. We thank member of the Stanford Genome Sequencing Services Center which is supported by NIH Grant # 1S10OD020141-01.

Nonstandard Abbreviations and Acronyms:

CAD	coronary artery disease
ECs	endothelial cells
MI	myocardial infarction
scRNAseq	single-cell RNA sequencing
LAD	left anterior descending artery
CX40	Connexin 40
P	postnatal day
UMAP	uniform manifold approximation and projection
CytoTRACE	cellular trajectory reconstruction analysis using gene counts and expression
DEGs	differentially expressed genes
VEGF	Vascular Endothelial Growth Factor

REFERENCES

1. Nowbar AN, Gitto M, Howard JP, Francis DP, Al-Lamee R. Mortality from ischemic heart disease: Analysis of data from the world health organization and coronary artery disease risk factors from NCD risk factor collaboration. Circ Cardiovasc Qual Outcomes. 2019;12:1–11.
2. Hulot J-S, Ishikawa K, Hajjar RJ. Gene therapy for the treatment of heart failure: promise postponed. Eur Heart J. 2016;37:1651–1658. [PubMed: 26922809]
3. Giordano FJ, Gerber HP, Williams SP, et al.cardiac myocyte vascular endothelial growth factor paracrine pathway is required to maintain cardiac function. Proc Natl Acad Sci U S A. 2001;98:5780–5785. [PubMed: 11331753]
4. Taimeh Z, Loughran J, Birks EJ, Bolli R. Vascular endothelial growth factor in heart failure. Nat Rev Cardiol. 2013;10:519–530. [PubMed: 23856679]
5. Rubanyi GM. Mechanistic, technical, and clinical perspectives in therapeutic stimulation of coronary collateral development by angiogenic growth factors. Mol. Ther2013;21:725–738. [PubMed: 23403495]
6. Schaper WCollateral circulation. Past and present. Basic Res. Cardiol2009;104:5–21. [PubMed: 19101749]
7. Simons M, Eichmann A. Molecular Controls of Arterial Morphogenesis. Circ Res. 2015;116:1712–1724. [PubMed: 25953926]
8. Chang A, Raftrey B, D'Amato G, et al.DACH1 stimulates shear stress guided endothelial cell migration and coronary artery growth through the CXCL12-CXCR4 signaling axis. Genes Dev. 2017;31:1308–1324. [PubMed: 28779009]
9. Red-Horse K, Ueno H, Weissman IL, Krasnow M a. Coronary arteries form by developmental reprogramming of venous cells. Nature. 2010;464:549–53. [PubMed: 20336138]
10. Su T, Stanley G, Sinha R, et al.Single-cell analysis of early progenitor cells that build coronary arteries. Nature. 2018;559:356–362. [PubMed: 29973725]
11. Das S, Goldstone AB, Wang H, et al.A Unique Collateral Artery Development Program Promotes Neonatal Heart Regeneration. Cell. 2019;176:1128–1142.e18. [PubMed: 30686582]
12. Renier N, Wu Z, Simon DJ, Yang J, Ariel P, Tessier-Lavigne M. iDISCO: A Simple, Rapid Method to Immunolabel Large Tissue Samples for Volume Imaging. Cell[Internet].2014 [cited 2014 Oct 30];159:896–910. Available from: http://linkinghub.elsevier.com/retrieve/pii/S0092867414012975 [PubMed: 25417164]
13. Stuart T, Butler A, Hoffman P, et al.Comprehensive Integration of Single-Cell Data. Cell. 2019;177:1888–1902.e21. [PubMed: 31178118]
14. Chen HI, Sharma B, Akerberg BN, et al.The sinus venosus contributes to coronary vasculature through VEGFC-stimulated angiogenesis. Development. 2014;141:4500–4512. [PubMed: 25377552]
15. Haefliger JA, Allagnat F, Hamard L, Le Gal L, Meda P, Nardelli-Haefliger D, Gnot E, Alonso F. Targeting Cx40 (Connexin40) expression or function reduces angiogenesis in the developing mouse retina. Arterioscler Thromb Vasc Biol. 2017;37:2136–2146. [PubMed: 28982669]
16. Pitulescu ME, Schmidt I, Giaimo BD, et al.Dll4 and Notch signalling couples sprouting angiogenesis and artery formation. Nat Cell Biol. 2017;19:915–927. [PubMed: 28714968]
17. Xu C, Hasan SS, Schmidt I, Rocha SF, Pitulescu ME, Bussmann J, Meyen D, Raz E, Adams RH, Siekmann AF. Arteries are formed by vein-derived endothelial tip cells. Nat Commun. 2014;5:5758. [PubMed: 25502622]
18. Vanlandewijck M, He L, Mäe MA, et al.A molecular atlas of cell types and zonation in the brain vasculature. Nature. 2018;554:475–480. [PubMed: 29443965]
19. Fang J, Hirschi K. Molecular regulation of arteriovenous endothelial cell specification. F1000Research. 2019;8:1–11.
20. Cao J, Spielmann M, Qiu X, et al.The single-cell transcriptional landscape of mammalian organogenesis. Nature. 2019;566:496–502. [PubMed: 30787437]
21. Gulati GS, Sikandar SS, Wesche DJ, et al.Single-cell transcriptional diversity is a hallmark of developmental potential. Science (80-). 2020;367:405–411.

22. Fang JS, Coon BG, Gillis N, Chen Z, Qiu J, Chittenden TW, Burt JM, Schwartz MA, Hirschi KK. Shear-induced Notch-Cx37-p27 axis arrests endothelial cell cycle to enable arterial specification. Nat Commun. 2017;8:2149. [PubMed: 29247167]

23. Herpers R, Van De Kamp E, Duckers HJ, Schulte-Merker S. Redundant roles for sox7 and sox18 in arteriovenous specification in Zebrafish. Circ Res. 2008;102:12–15. [PubMed: 18032732]

24. Cardoso AC, Lam NT, Savla JJ, et al.Mitochondrial substrate utilization regulates cardiomyocyte cell-cycle progression. Nat Metab[Internet].2020;2:167–178. Available from: 10.1038/s42255-020-0169-x [PubMed: 32617517]

25. Red-Horse K, Siekmann AF. Veins and Arteries Build Hierarchical Branching Patterns Differently: Bottom-Up versus Top-Down. BioEssays. 2019;41:1800198.

26. Chen HI, Poduri A, Numi H, et al.VEGF-C and aortic cardiomyocytes guide coronary artery stem development. J Clin Invest. 2014;1–16.

27. Sörensen I, Adams RH, Gossler A. DLL1-mediated Notch activation regulates endothelial identity in mouse fetal arteries. Blood. 2009;113:5680–5688. [PubMed: 19144989]

28. Miquerol L, Thireau J, Bideaux P, Sturny R, Richard S, Kelly RG. Endothelial plasticity drives arterial remodeling within The endocardium after myocardial infarction. Circ Res. 2015;116:1765–1771. [PubMed: 25834185]

29. Zudaire E, Gambardella L, Kurcz C, Vermeren S. A computational tool for quantitative analysis of vascular networks. PLoS One. 2011;6:1–12.

30. McInnes L, Healy J, Melville J. UMAP: for Dimension Reduction. 2018;Available from: http://arxiv.org/abs/1802.03426

31. Tirosh I, Izar B, Prakadan SM, et al.Dissecting the multicellular ecosystem of metastatic melanoma by single-cell RNA-seq. Science (80-). 2016;352:189–196.

32. Roostalu U, Thisted L, Skytte JL, et al.Effect of captopril on post-infarction remodelling visualized by light sheet microscopy and echocardiography. Sci Rep[Internet].2021;11:1–13. Available from: 10.1038/s41598-021-84812-7 [PubMed: 33414495]

NOVELTY AND SIGNIFICANCE

What Is Known?

- Dach1 knockout mice have impaired embryonic coronary artery development.
- Growth of coronary arteries is a proposed way to protect against myocardial infarction

What New Information Does This Article Contribute?

- Overexpression of Dach1 increased artery endothelial specification during embryonic and postnatal development.
- Single cell RNA sequencing showed that Dach1 reduced lipid transport associated genes as part of its differentiation program.
- Adult Dach1 overexpression mice had increased survival and heart function after myocardial infarction

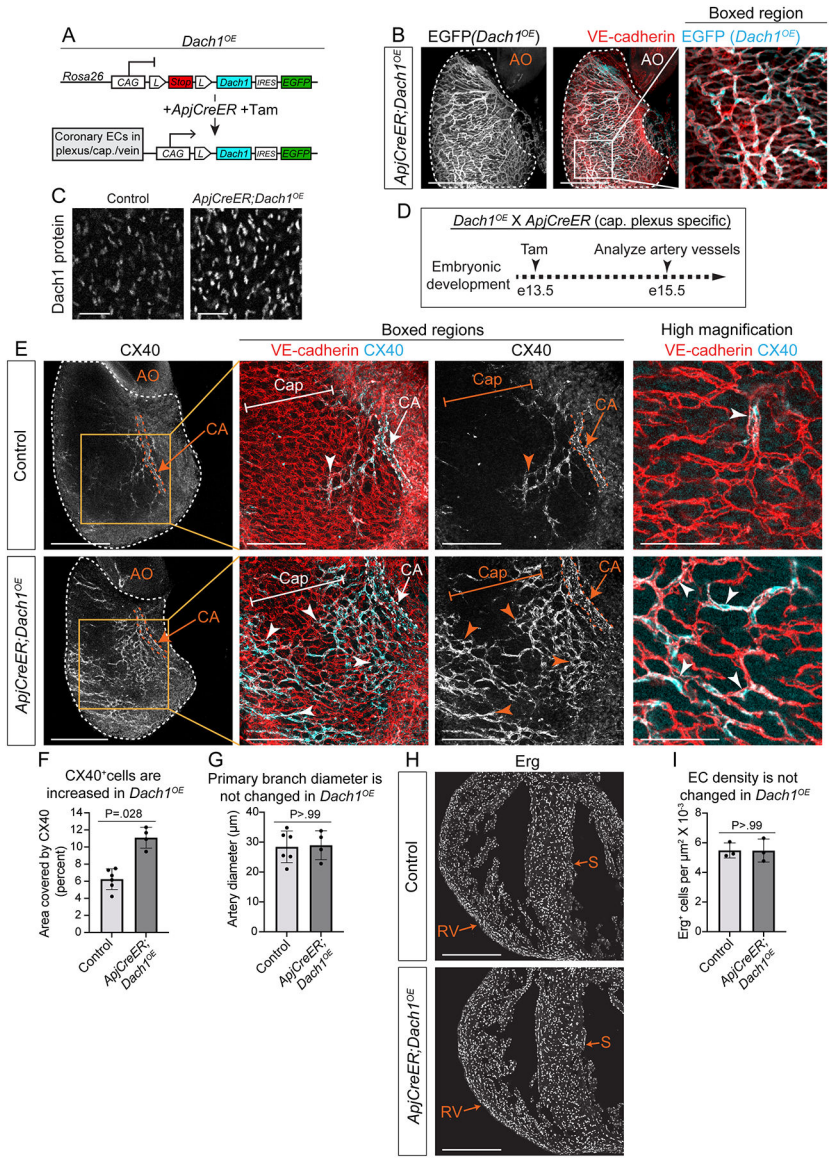

Figure 1. *Dach1*^{OE} increases artery specification during coronary artery development.

A) *Dach1*^{OE} transgenic mouse line. **B**) Confocal image of an *ApjCreER;Dach1*^{OE} mouse heart (e15.5) immunostained for EGFP to assess recombination rate in the transgenic line. **C**) Dach1 immunostaining in *Dach1*^{OE} hearts. **D**) Experimental strategy in **E**-**I**. **E**) E15.5 hearts imaged on the right lateral side show an increase in CX40 staining in *Dach1*^{OE} capillaries (arrowheads). **F)** Quantification of the percent heart area immunostained by CX40 (n=6 control, n=4 *Dach1*^{OE}; Mann-Whitney test; Holm-Sidak adjusted p-value from testing three hypotheses). **G)** Quantification of primary artery diameters in e15.5 hearts (n=6 control, n=4 *Dach1*^{OE}, Mann-Whitney test; Holm-Sidak adjusted p-value from testing three hypotheses). **H**) Erg immunostaining e15.5 heart sections. **I**) Quantification of endothelial density (n=3 control, n=3 *Dach1*^{OE}, Mann-Whitney test; Holm-Sidak adjusted p-value from testing three hypotheses). AO= Aorta, CA= Coronary Artery, Cap= Capillary S= Septum, RV= Right Ventricle. Scale bar= 400 μM in B), E) (whole heart), and H). Scale bar= 200μM

in E) (boxed area). Scale bar= 100μM in E) highest magnification. Scale bar= 50μM in C). All data represent mean+-SD.

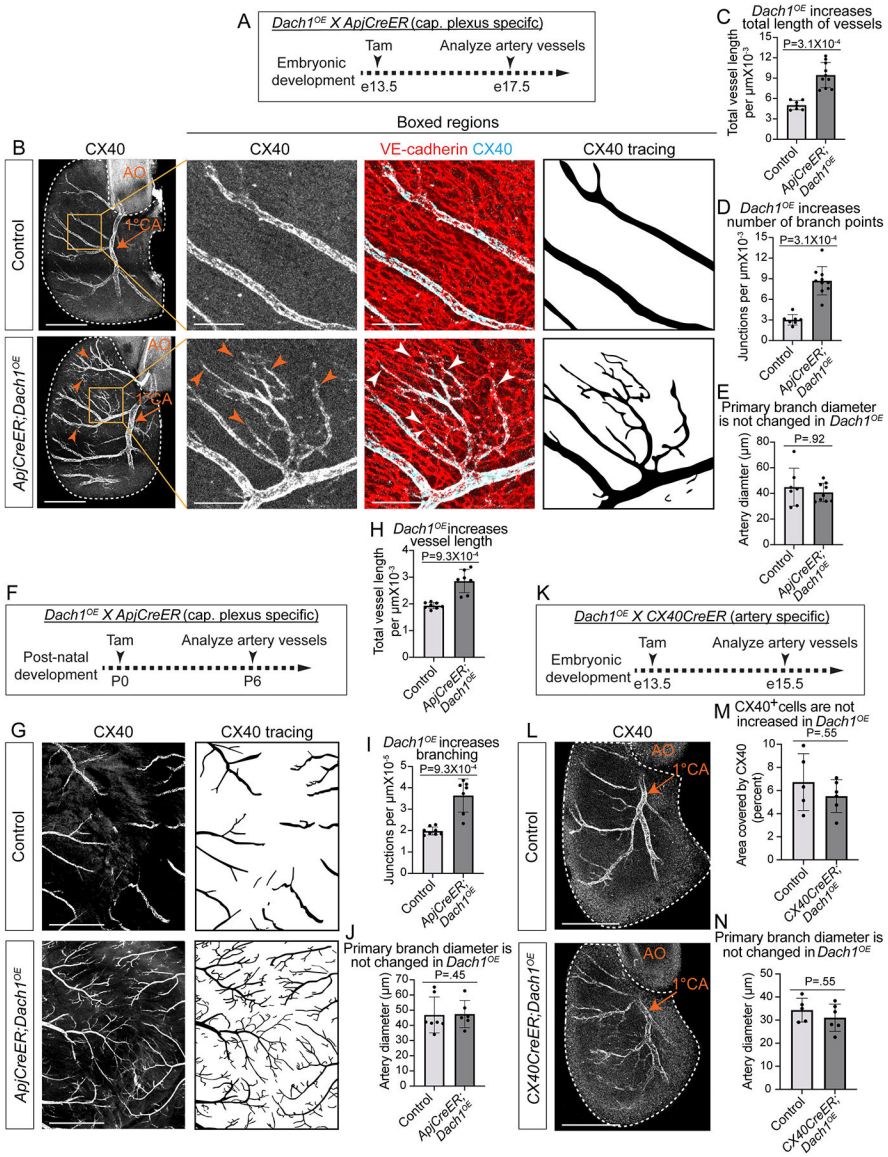

Figure 2. *Dach1*^{OE} increases coronary artery branching.

A) Experimental strategy in **B**-**E**. **B**) Right lateral view of e17.5 hearts. Arrowheads indicate extra artery branches. Boxed regions show the scale of extra CX40^{+} vessels and the normal capillary bed morphology in *Dach1*^{OE}. **C**-**E**) Quantification of the total length (**C**) (n=7 control, n=10 *Dach1*^{OE}; Mann-Whitney test; Holm-Sidak adjusted p-value from testing three hypotheses) and number of branch points (**D**) (n=7 control, n=10 *Dach1*^{OE}; Mann-Whitney test; Holm-Sidak adjusted p-value from testing three hypotheses) in the CX40^{+} vessel network, and primary coronary artery diameters (**E**) in e17.5 hearts (n=7 control, n=9 *Dach1*^{OE}, Mann-Whitney test; Holm-Sidak adjusted p-value from testing three hypotheses). **F**) Experimental strategy in **G**-**J**. **G**) CX40 immunostaining of the ventral surface of postnatal hearts shows increased branching in *Dach1*^{OE}. **H** and **I**) Quantification of the total length (**H**) and branch points (**I**) of CX40^{+} vessels, and **J**) measurement of main coronary artery diameters in postnatal hearts (n=7 control, n=6 *Dach1*^{OE}, Mann-Whitney test; Holm-

Sidak adjusted p-value from testing three hypotheses). **K**) Experimental strategy to generate artery specific *Dach1*^{OE} expression using *Cx40CreER*. **L**) CX40 immunostaining of control and *CX40CreER;Dach1*^{OE} hearts. **M** and **N**) Quantification of CX40^{+} area (**M**) and artery diameter (**N**) (n=5 control, n=6 *Dach1*^{OE}, Mann-Whitney test; Holm-Sidak adjusted p-value from testing two hypotheses). AO= Aorta, CA= Coronary Artery. Scale bar= 500μM in G). Scale bar= 400μM in B) (entire heart) and L). Scale bar= 200μM in B) (boxed region). All data represent mean+-SD.

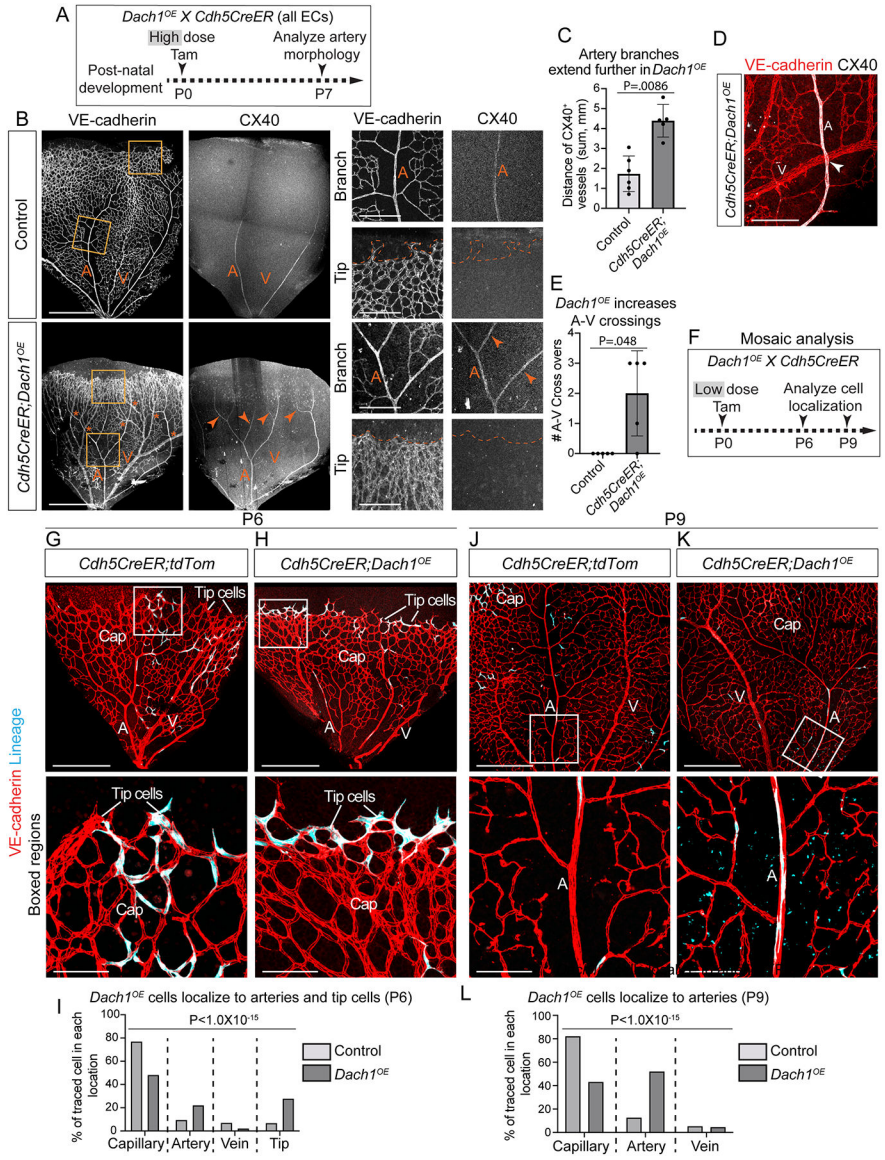

Figure 3. *Dach1*^{OE} increases retinal arterialization and promotes endothelial cell migration into arteries.

A) Dosing strategy for retina vasculature analysis. **B**) Retinas from *Dach1*^{OE} pups contained increased number of CX40+ vessel branches (arrowheads) and artery-vein crossing (asterisks). Right panels show insets indicated by dashed boxes. **C**) The total length of all CX40^{+} vessels per retina was greater in *Dach1*^{OE} (n=6 control, n=5 *Dach1*^{OE}, Mann-Whitney test; Holm-Sidak adjusted p-value from testing two hypotheses). **D** and **E**) Image (**D**, arrowheads) and quantification (**E**) of artery-vein crossovers in *Dach1*^{OE} retinas (n=5 control, n=5 *Dach1*^{OE}, Mann-Whitney test; Holm-Sidak adjusted p-value from testing two hypotheses). **F**) Experimental strategy in **G**-**L**. (**G**-**L**) Images (**G**, **H**, **J**, and **K**) and quantification (**I** and **L**) of control or *Dach1*^{OE} cells in retinas from the indicated ages. Boxed regions highlight the tip and capillary cells (**G** and **H**) or artery (**J** and **K**) where there was a differential localization of control and *Dach1*^{OE} cells. (**I**: n=1020 control, n=767 *Dach1*^{OE}, Chi-square test; **L**: n=1708 control, n=540 *Dach1*^{OE}, Chi-square test). A= Artery,

V= Vein, Cap=Capillary. Scale bar= 400μM in B), G), H), J), and K) (full view). Scale bar= 200μM in D), B) (close up). Scale bar= 100μM in G), H), J), and K) (close up). all data are mean+-SD.

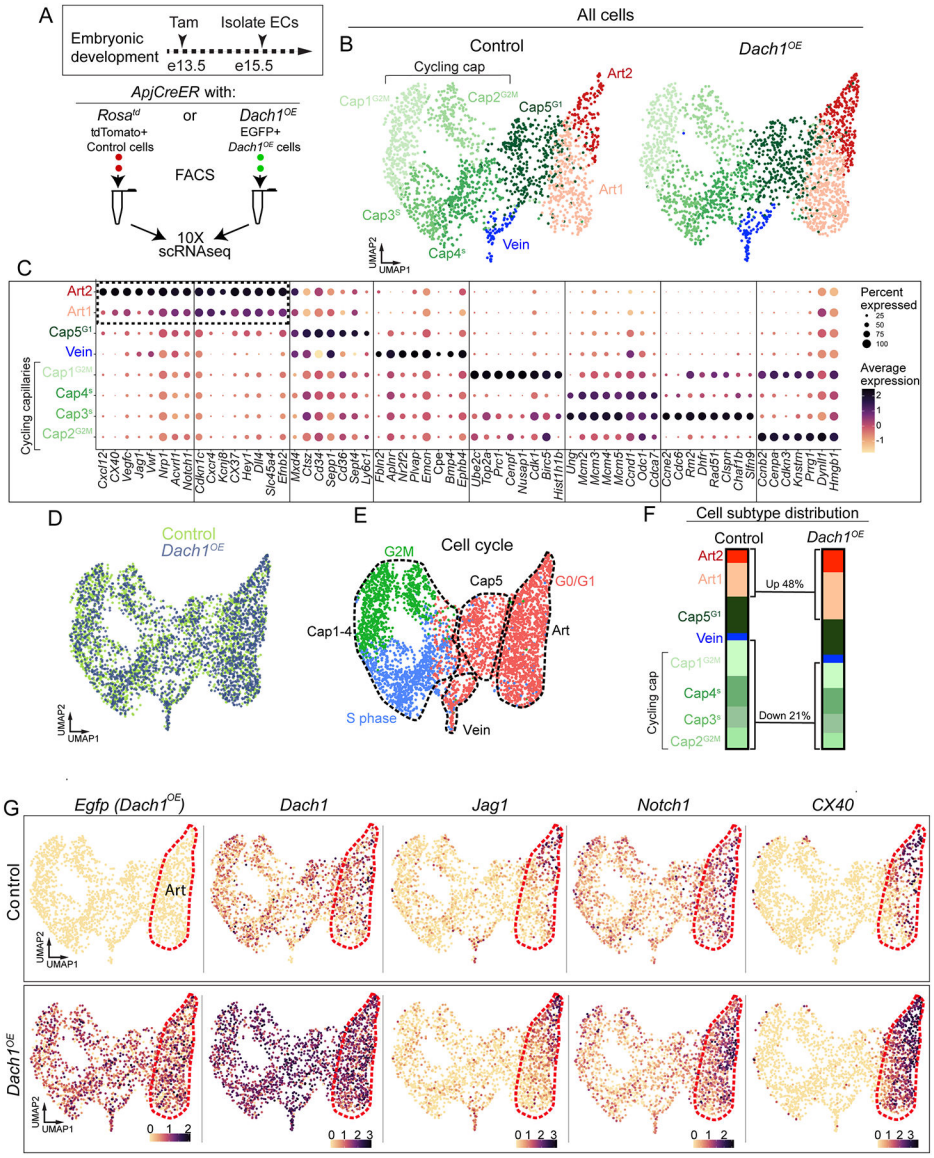

Figure 4. Single cell RNA sequencing of endothelial cells in *Dach1*^{OE} hearts.

A) Littermate e15.5 embryos expressing *ApjCreER* with either *Rosa26tdTomato* or *Rosa26Dach1*^{OE} were FACS sorted to isolate coronary endothelial cells for single cell sequencing. **B**) UMAP projections of data showed 8 endothelial cell clusters. **C**) The genes that define each cluster are plotted with their relative expression in each cluster. Boxed region highlights Art1 and Art2 signature genes, which are similar but with increased expression in Art2. Differential gene expression between clusters was found using the Wilcoxon Rank Sum Test. **D**) UMAP plot showing that cells from both genotypes overlapped; *Dach1*^{OE} did not produce a new subtype. **E**) UMAP plots with both genotypes combined showing cell cycle stage using the CellCycleScoring function in seurat. **F**) Percent of cells in each cluster for both genotypes. **G**) Scaled expression of the *Dach1*^{OE} transgene, *Dach1*, and select artery markers.

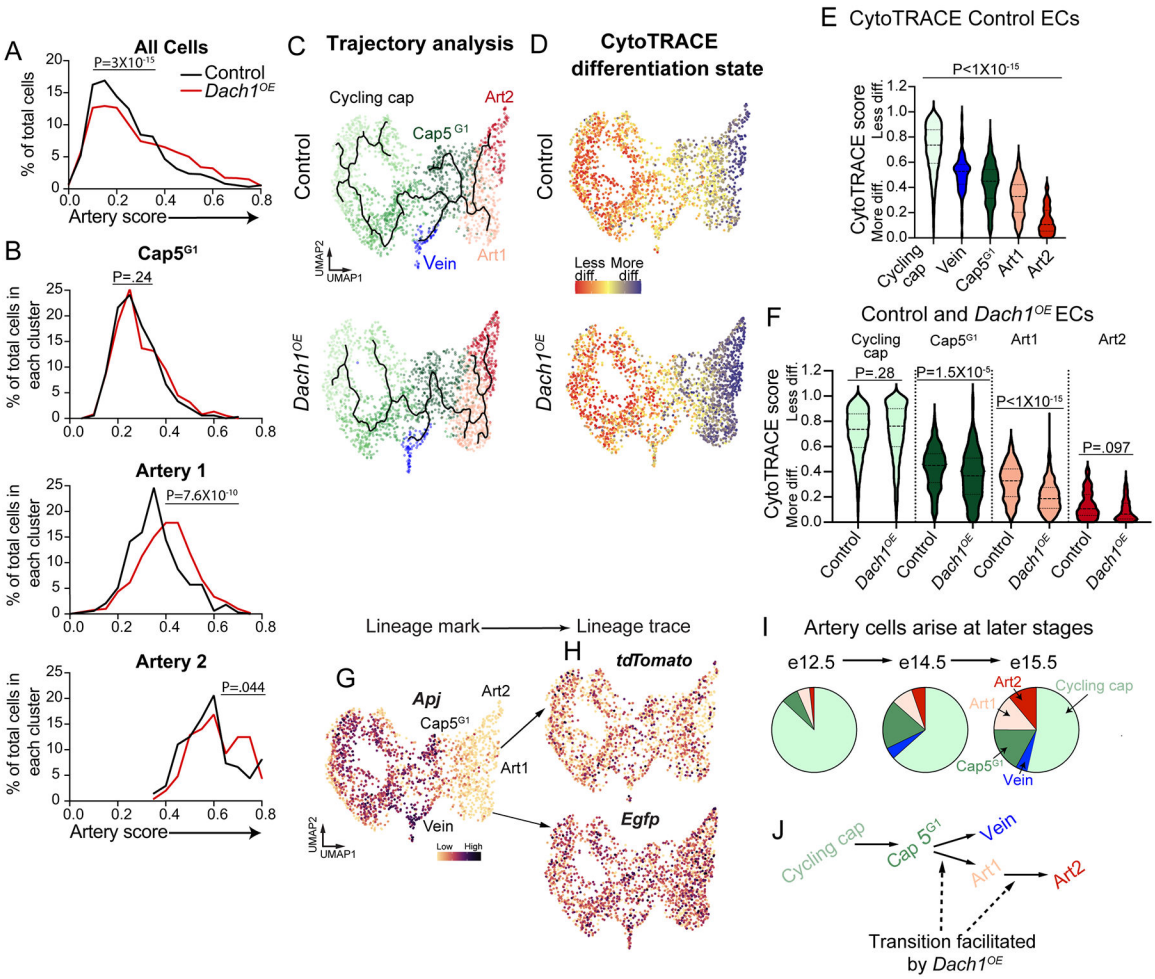

Figure 5. Dach1 enhances artery specification in endothelial cells.

A) Calculating an artery score for each cell (see methods) revealed that *Dach1*^{OE} shifted the total distribution of cells to a higher artery score (control= 1975 cells, *Dach1*^{OE}= 2149 cells, Mann-Whitney test). (**B**) Within each individual cluster, only the Art1 and Art2 clusters had significant shifts in artery score. (post-hoc Bonferroni multiple comparison test following two way ANOVA) **C)** Cell trajectories (solid line) from either genotype inferred using Monocle3. **D**) CytoTRACE differentiation scores for each cell displayed on the UMAP plot. **E**) CytoTRACE scored calculated for controls cells (one way ANOVA). **F**) CytoTRACE scores were lower (more differentiated) for Cap5^{G1} and Art1in *Dach1*^{OE} (post-hoc Bonferroni multiple comparison test following two way ANOVA). **G**) *Apj*, the enhancer/promoter used to drive Cre, is expressed in all endothelial cells except arteries. **H**) The lineage traces from *ApjCreER* (*tdTomato* or *Dach1*^{OE}*-EGFP*) are later expressed in the arterial endothelial cells. **I**) Graphs showing the percent of cells in each indicated cluster in analogous coronary endothelial cell scRNAseq datasets from indicated embryonic days (e). **J**) Model for cell differentiation trajectory during coronary artery development and the proposed influence of Dach1. Box plots are mean+-SD.

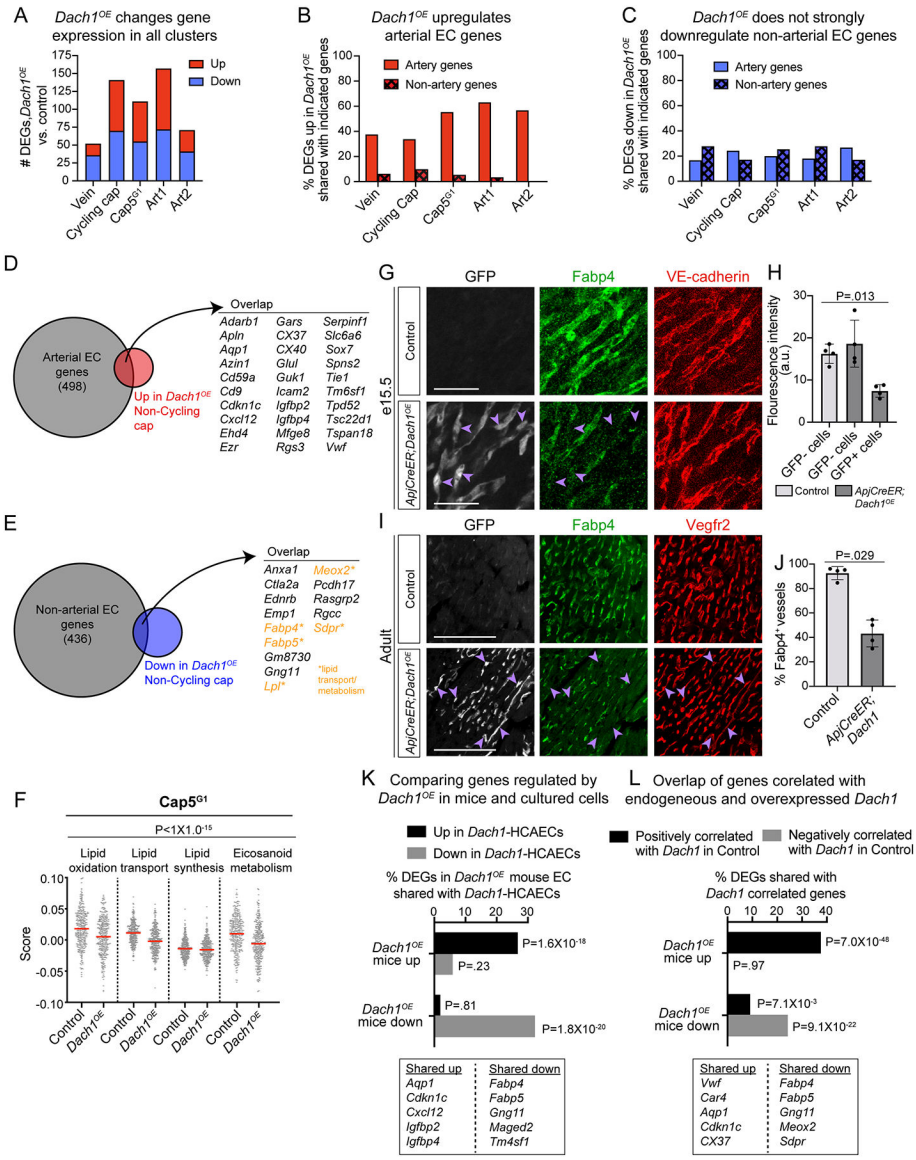

Figure 6. Specific gene expression changes in *Dach1*^{OE}.

A) The number of differentially expressed genes (DEGs) when separately comparing control and *Dach1*^{OE} cells from each cluster. **B** and **C**) Genes that are either positively or negatively enriched in control artery clusters we identified and termed “artery genes” and “non-artery genes”, respectively. DEGs that were either up- or down-regulated by *Dach1*^{OE} in each cluster were then compared to these lists. Upregulated DEGs in *Dach1*^{OE} have strong overlap with artery genes (**B**) while downregulated DEGs in *Dach1*^{OE} have less overlap with non-artery genes (**C**). **D** and **E**) Venn diagrams showing overlap of artery (**D**) and non-artery (**E**) genes with DEGs either up- or down-regulated by *Dach1*^{OE} in non-cycling capillary. **F**) Cell scores generated for select lipid pathways (see methods) showed a reduction in *Dach1*^{OE} Cap5^{G1} (2 way ANOVA, p-value represents genotype factor). **G-J**) Validation of decreased Fabp4 in *Dach1*^{OE} cells using immunofluorescence on hearts at e15.5 (n=4 per group, Kruskal-Wallis test). **(G** and **H)** or adult stages (n=4 control, n=4

Dach1^{OE}, Mann-Whitney test). **(I** and **J)**. Purple arrowheads show GFP^{+}Fabp4^{-} cells in **(G)** and **(I)**. **K**) DEGs shared between endothelial cells experiencing *Dach1* overexpression in either developing mouse hearts (*Dach1*^{OE}) or primary cell culture (*Dach1*-HCAECs) (hypergeometric test). **L**) Overlap between mouse *Dach1*^{OE} DEGs and genes that are positively or negatively correlated with endogenous *Dach1* in scRNAseq data from control hearts (hypergeometric test). Scale bar= 50μM in G). Scale bar= 100μM in I). Red bar= mean in (F), data represent mean +-SD in (H and J).

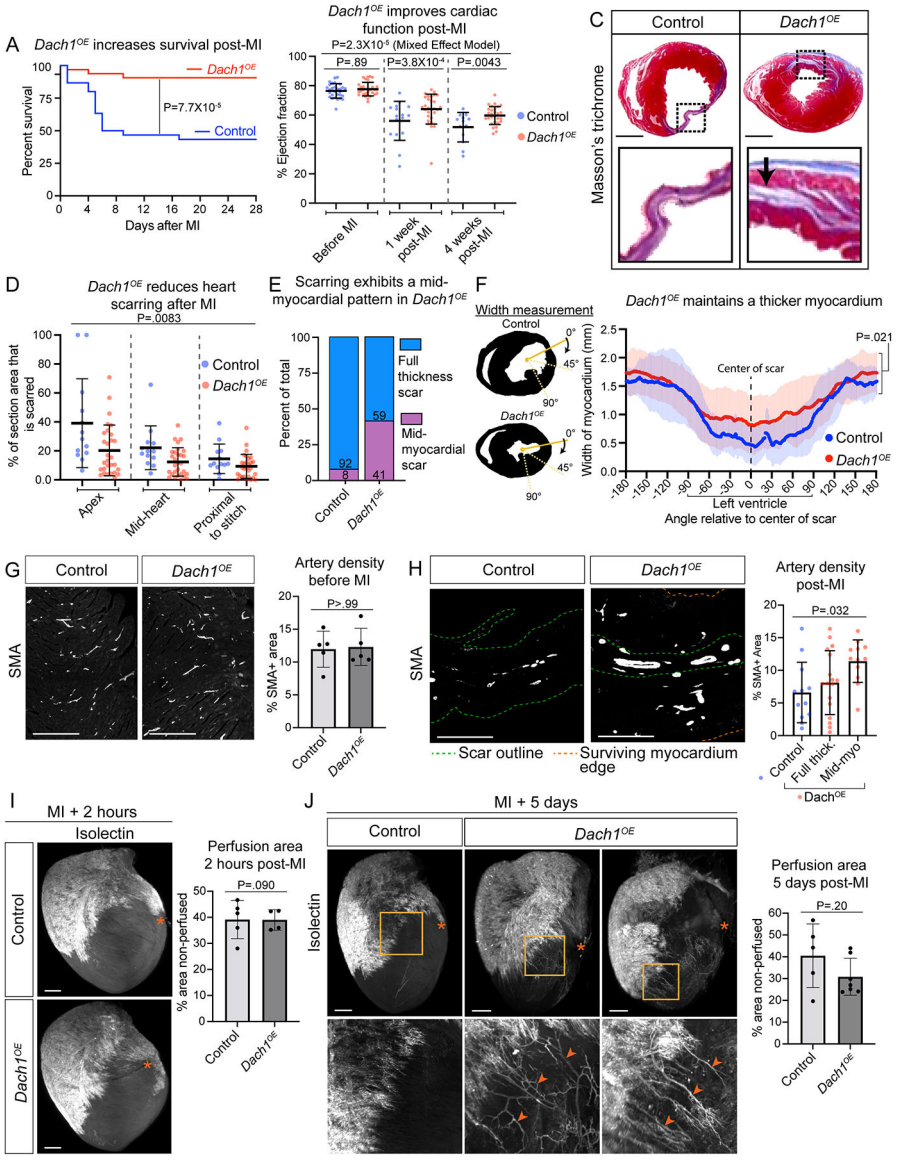

Figure 7. *Dach1* overexpression promotes survival after myocardial infarction.

A) Survival curve during 4-weeks post-MI. (n=30 control, n=32 *Dach1*^{OE}; Log-rank test) **B**) Percent ejection fraction at the indicated time points (n=29 control, n=30 *Dach1*^{OE}; above graph: mixed effect model above (p-value represents genotype factor); individual comparisons: Holm-Sidak adjusted p-values). **C**) Hematoxylin & Eosin staining on representative hearts. Arrow highlight an example of a mid-myocardial scar. **D)** Percent of total myocardium stained with Masson's Trichrome in sections from three levels posterior to the ligation (n=13 control, n=29 *Dach1*^{OE}; Mixed effect model, p-value represents genotype factor). **E)** Quantification of scarring pattern. **F)** The width of the myocardium at 360 angles around the heart. In the left ventricle where the infarct was induced, *Dach1*^{OE} better preserved myocardial thickness when compared to controls. Lines are averages of each group while shading indicates S.D. (n=13 control and n=29 *Dach1*^{OE}; Mixed effect model, p-value represents genotype factor) **G** and **H)** Smooth muscle actin (SMA) staining

in sections from uninjured (**G**) (n=5 control, n=5 *Dach1*^{OE}; Mann-Whitney test) and post-MI hearts (H) (n=12 control, n=29 *Dach1*^{OE}; One-way ANOVA) with quantification of SMA density. **I** and **J)** Isolectin perfusion 2 hours (n=5 control, n=4 *Dach1*^{OE}; Mann-Whitney test) or 5 days (n=5 control, n=7 *Dach1*^{OE}; Mann-Whitney test) after MI, asterisks indicate stitch location. Arrows show perfused vessels connecting from perfused regions into the infarct zone in *Dach1*^{OE}. Scale bar=1mm in (C), (I), (J). Scale bar= 500μm in (G). Scale bar= 250 in (H). Error bars show mean+-SD.